An optical-sensing modality that exploits Dyakonov–Tamm waves

Farhat Abbas,[1] Akhlesh Lakhtakia,[2] Qaisar A. Naqvi,[1] and Muhammad Faryad[3,*]

[1]*Department of Electronics, Quaid-i-Azam University, Islamabad 45320, Pakistan*
[2]*Department of Engineering Science and Mechanics, Pennsylvania State University, University Park, Pennsylvania 16802, USA*
[3]*Department of Physics, Lahore University of Management Sciences, Lahore 54792, Pakistan*
**Corresponding author: muhammad.faryad@lums.edu.pk*

Received October 14, 2014; revised November 5, 2014; accepted November 5, 2014; posted November 25, 2014 (Doc. ID 224528); published December 17, 2014

Surface-wave-based optical sensing of an analyte in a fluid relies on the sensitivity of the surface wave to the electromagnetic properties of the analyte-containing fluid in the vicinity of the guiding interface. Surface-plasmon-polariton (SPP) waves are most commonly used for optical sensing because of the ease of the excitation of an SPP wave when the fluid is partnered with a metal. If the fluid is replaced by a porous, anisotropic, and periodically nonhomogeneous solid filled with the fluid, while the metal is replaced by an isotropic homogeneous dielectric material, the surface wave is called a Dyakonov–Tamm (DT) wave. We have theoretically determined that the incorporation of the DT-waveguiding interface in a prism-coupled configuration provides an alternative to the analogous SPP wave-based sensor, with comparable dynamic sensitivity.

OCIS codes: (240.0310) Thin films; (240.6690) Surface waves; (310.2785) Guided wave applications.
http://dx.doi.org/10.1364/PRJ.3.000005

1. INTRODUCTION

Any electromagnetic surface wave propagates bound to an interface of two dissimilar materials [1,2]. This localization of the surface wave to the interface allows its use in optical sensing, because a small change in the electromagnetic properties of either of the two partnering materials near the interface can result in a significant change in the characteristics of the surface wave.

Surface-plasmon-polariton (SPP) waves are extensively used for optical sensors [3–7]. The propagation of an SPP wave is guided by the interface of a metal and a dielectric material. Although the partnering dielectric material is usually a fluid containing the analyte to be sensed [3–6], it can also be a porous material that is infiltrated by the analyte-containing fluid [8]. Interestingly, the experimentally measured dynamic sensitivity of a prism/metal/fluid-infiltrated porous material/fluid setup [8] has been found to significantly exceed the theoretical sensitivity of the prism/metal/fluid setup [4].

A surface wave called the Tamm wave is guided by the interface of two isotropic dielectric materials, at least one of which is periodically nonhomogeneous in the direction perpendicular to the interface [9,10]. The Tamm wave has also been experimentally exploited for optical sensing, with the analyte-containing fluid partnering a periodically stratified solid material [11–13].

Surface waves called Dyakonov–Tamm (DT) waves were theoretically predicted a few years ago [14]. Guided by the interface of two dielectric materials of which at least one is both anisotropic and periodically nonhomogeneous normal to the interface [2], DT waves were experimentally observed very recently [15,16].

Not surprisingly, DT waves should also be useful for optical sensing. In the initial proposal [17], the commonplace prism-coupled configuration [2,5,6] was adopted. A monochromatic collimated light beam is supposed to be incident on one of the two slanted faces of a prism made of a material with a sufficiently high refractive index n_{prism}. The base of the prism is coated with a chiral sculptured thin film (STF) [18], which is a porous, anisotropic, and periodically nonhomogeneous material. When the chiral STF contacts the analyte-containing fluid, their interface can guide a DT wave [17]. The chiral STF functions as an anisotropic and periodically nonhomogeneous partner, while the fluid is the isotropic and homogeneous partner. The intensity of light exiting the second slanted face of the prism is recorded as the angle of incidence θ_{inc} on the base of the prism is varied by changing the direction of propagation of the light beam incident on the first slanted face of the prism. A pronounced and rather narrow dip in the recorded intensity can indicate the excitation of a DT wave.

As the analyte-containing fluid also infiltrates the chiral STF due to its porosity, the proposed sensor should be quite sensitive as changes in the concentration of the analyte will affect the dielectric properties of both partnering materials. However, this sensing modality does not offer flexibility in the choice of the partnering isotropic dielectric material.

In this paper, we focus our attention on a new sensing modality exploiting the DT-wave phenomenon. As shown in Fig. 1(a), a nonporous layer of thickness L_d and made of an isotropic material of refractive index n_d is interposed between the prism and the chiral STF. With a proper choice of n_d, it would be possible to excite a DT wave guided by the interface of the nonporous solid material and the

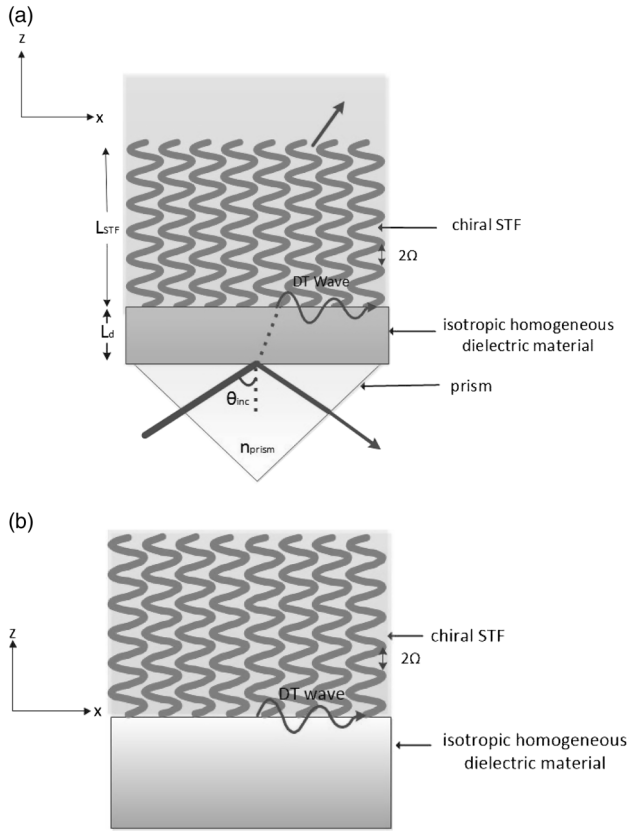

Fig. 1. Schematic representations: (a) proposed optical-sensing modality, and (b) underlying canonical boundary-value problem.

fluid-infiltrated chiral STF, rather than the interface of the fluid-infitrated chiral STF and the fluid. A short description of the model used for the fluid-infiltrated chiral STF is presented in Section 2 and the numerical results are presented and discussed in Section 3. Concluding remarks are presented in Section 4.

2. FLUID-INFILTRATED CHIRAL STF

A schematic of the canonical boundary-value problem underlying the sensing modality proposed in this paper is shown in Fig. 1(b). The half space $z < 0$ is occupied by the isotropic partner of refractive index n_d, and the half-space $z > 0$ is occupied by the chiral STF infiltrated with an analyte-containing fluid of refractive index n_ℓ. A change in analyte concentration would alter n_ℓ.

Essentially, a chiral STF is fabricated by obliquely directing a collimated vapor flux under low pressure onto a uniformly rotating substrate [18]. The angle between the direction of the vapor flux and the substrate is denoted by $\chi_v \in (0°, 90°]$. Under suitable conditions, an assembly of parallel nanohelixes form, with the helical axes perpendicular to the substrate. The porosity and morphology of a chiral STF can be tailored during fabrication [18].

The relative permittivity dyadic of a chiral STF can be stated as [18]

$$\underline{\underline{\varepsilon}}_{\rm STF}(z) = \underline{\underline{S}}_z(z) \cdot \underline{\underline{S}}_y(\chi) \cdot (\varepsilon_a \hat{\mathbf{z}}\,\hat{\mathbf{z}} + \varepsilon_b \hat{\mathbf{x}}\,\hat{\mathbf{x}} + \varepsilon_c \hat{\mathbf{y}}\,\hat{\mathbf{y}}) \cdot \underline{\underline{S}}_y^T(\chi) \cdot \underline{\underline{S}}_z^T(z), \quad (1)$$

where the superscript T denotes the transpose; the dyadic

$$\underline{\underline{S}}_z(z) = (\hat{\mathbf{x}}\,\hat{\mathbf{x}} + \hat{\mathbf{y}}\,\hat{\mathbf{y}}) \cos(h\pi z/\Omega) + (\hat{\mathbf{y}}\,\hat{\mathbf{x}} - \hat{\mathbf{x}}\,\hat{\mathbf{y}}) \sin(h\pi z/\Omega) + \hat{\mathbf{z}}\,\hat{\mathbf{z}} \quad (2)$$

involves 2Ω as the helical pitch and either $h = +1$ for structural right-handedness or $h = -1$ for structural left-handedness; and the dyadic

$$\underline{\underline{S}}_y(\chi) = (\hat{\mathbf{x}}\,\hat{\mathbf{x}} + \hat{\mathbf{z}}\,\hat{\mathbf{z}}) \cos\chi + (\hat{\mathbf{z}}\,\hat{\mathbf{x}} - \hat{\mathbf{x}}\,\hat{\mathbf{z}}) \sin\chi + \hat{\mathbf{y}}\,\hat{\mathbf{y}} \quad (3)$$

contains $\chi \in [0°, 90°]$ as the angle of rise of the nanohelixes. Both χ and the scalars ε_a, ε_b, and ε_c depend on the angle χ_v as well as on the evaporated material. Furthermore, $\varepsilon_{a,b,c}$ also depend on the free-space wavelength λ_0 and n_ℓ. Each nanohelix can be viewed as a string of highly elongated ellipsoidal inclusions, which permits the use of homogenization theory to predict the effective relative permittivity dyadic of a fluid-infiltrated chiral STF from the effective relative permittivity dyadic of an uninfiltrated chiral STF [2,19].

3. ILLUSTRATIVE NUMERICAL RESULTS AND DISCUSSION

For all numerical results presented here, we fixed $\lambda_0 = 633$ nm, $n_{\rm prism} = 2.6$, $\chi_v = 15°$, and $\Omega = 197$ nm. We chose magnesium flouride ($n_d = 1.377$ [15]) as the isotropic dielectric partner. We used the forward and inverse Bruggeman homogenization formalisms in the manner detailed elsewhere [19] to estimate $\varepsilon_{a,b,c}$ for the chiral STF infiltrated with a fluid of refractive index $n_\ell \in [1, 1.5]$ by taking measured data for a columnar thin film made by evaporating patinal titanium oxide [20]. Also, consistently with predecessor works [14,17,19], we used $\chi = 37.6745°$; furthermore, we fixed $\varepsilon_a = 2.13952$, $\varepsilon_b = 3.66907$, and $\varepsilon_c = 2.82571$ when $n_\ell = 1$.

Let us begin with the canonical boundary-value problem depicted in Fig. 1(b), because it provides predictions for the prism-coupled configuration of Fig. 1(a). Without significant loss of generality and for the sake of illustration, we let the DT wave propagate along the x axis with an $\exp(iqx)$ dependence. Adopting the theoretical formalism described elsewhere [2,14] for the dependence on z, we obtained a dispersion equation for the relative wavenumber q/k_0, where $k_0 = 2\pi/\lambda_0$ is the free-space wavenumber. The computed values of q/k_0 are presented in Fig. 2 against the refractive index n_ℓ of the fluid infiltrating the void regions of the chiral STF.

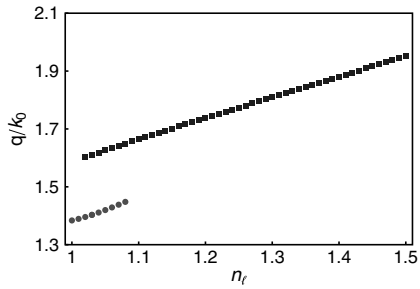

Fig. 2. Values of relative wavenumbers q/k_0 of DT waves guided by the interface of magnesium fluoride ($n_d = 1.377$) and the chosen titanium-oxide chiral STF infiltrated by a fluid of refractive index n_ℓ. In Figs. 2–4, the blue and red curves represent different DT waves.

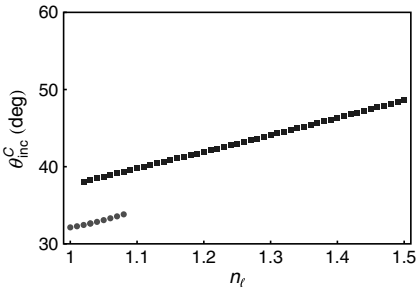

Fig. 3. Values of the angle of incidence θ_{inc}^{C} in the prism-coupled configuration in relation to the refractive index n_ℓ of the fluid infiltrating the chiral STF, as predicted by the canonical boundary-value problem.

For a specific $n_\ell \in [1, 1.5]$, the chosen interface supports either one or two DT waves, represented by the blue and red curves in Fig. 2. Both of these waves have different phase speeds, spatial profiles, and degree of localization to the interface between the partnering materials. No polarization state can be assigned to either of the two DT waves, because of the rotational nonhomogeneity of the chiral STF (i.e., Section 1.7.4 of [2]).

In Fig. 2, q is purely real. If the dielectric material of refractive index n_d were to be replaced by a metal, the DT waves would be replaced by SPP waves with complex q [2,19]. SPP waves attenuate during propagation, but ideally DT waves do not.

In the prism-coupled configuration, a DT wave is excited when the absorptance as a function of the incidence angle θ_{inc} (1) has a peak that is independent of the thicknesses of the partnering dielectric materials beyond threshold values, and (2) the absorptance peak's angular position is the same as the prediction $\theta_{\text{inc}}^{C} = \sin^{-1}(q/k_0 n_{\text{prism}})$ from the underlying canonical boundary-value problem [2,14]. Figure 3 shows θ_{inc}^{C} predicted as a function of n_ℓ. All of the values of θ_{inc}^{C} are practically convenient as they lie between 30° and 50°.

The dynamic sensitivity $\rho = d\theta_{\text{inc}}^{C}/dn_\ell$ is the change in the angular position of the absorptance peak in the prism-coupled configuration due to change in the refractive index n_ℓ of the fluid infiltrating the chiral STF. The predicted values of ρ versus n_ℓ are presented in Fig. 4. A comparison of the sensitivity ρ of DT waves in Fig. 4 with that of SPP waves using the same prism and the same chiral STF [19] indicates that the sensitivity of DT waves is generally similar to that of SPP waves. For the SPP waves, by using aluminum instead of magnesium fluoride, ρ lies between 22° and 32° per refractive index unit (RIU). For the DT waves studied in this paper, ρ lies between 14° and 27° per RIU.

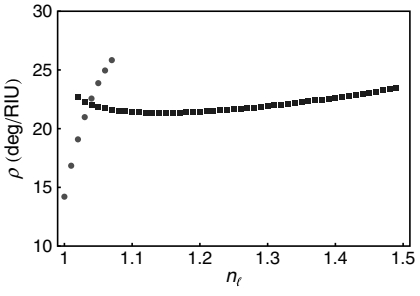

Fig. 4. Dynamic sensitivity ρ as a function of n_ℓ in the prism-coupled configuration computed from the predicted data presented in Fig. 3.

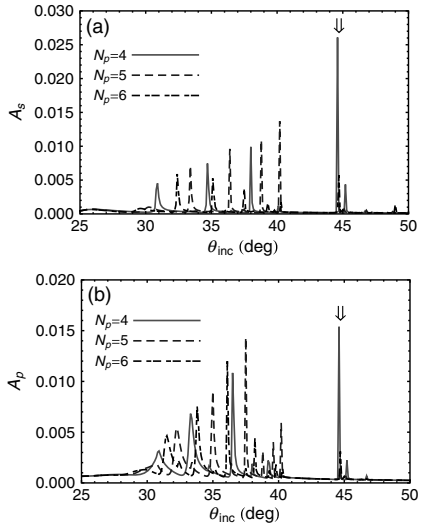

Fig. 5. Absorptances (a) A_s and (b) A_p plotted as functions of θ_{inc} for $N_p = L_{\text{STF}}/2\Omega \in \{4, 5, 6\}$, when $n_\ell = 1.33$, $\chi_v = 15°$, $L_d = 200$ nm, and $n_d = 1.377 + 10^{-4}i$. Downward arrows indicate the peaks that represent the excitation of DT waves.

Let us now present the actual results of the prism-coupled configuration, the algorithm for the computations being explained in detail elsewhere [2]. The light incident on the base of the prism is assumed to have an electric field of unit magnitude. For $\theta_{\text{inc}} > \sin^{-1}(n_\ell/n_{\text{prism}})$, there can be no transmittance in the fluid on top of the fluid-infitrated chiral STF in Fig. 1(a), so that the absorptance and the reflectance (calculated at the base of the prism) must add up to unity. In the plots of absorptance A versus the incidence angle θ_{inc}, the excitation of a DT wave is indicated by a peak that is independent of the thicknesses of the partnering dielectric materials beyond threshold values. The thickness-dependent peaks could indicate the excitation of waveguide modes [8,21].

Figure 5 presents the absorptances A_s and A_p for incident s- and p-polarized light, respectively, when $n_\ell = 1.33$, $\chi_v = 15°$, $L_d = 200$ nm, and $N_p = L_{\text{STF}}/2\Omega \in \{4, 5, 6\}$. For these calculations, we set $n_d = 1.377 + 10^{-4}i$. The tiny imaginary part was added to get nonzero values of the absorptances [17].

When $n_\ell = 1.33$, there can be no transmission for $\theta_{\text{inc}} \geq 30.8°$; furthermore, Fig. 3 indicates that the canonical boundary-value problem predicts the excitation of one DT wave at $\theta_{\text{inc}}^{C} = 44.8°$ in the prism-coupled configuration. In Fig. 5(a), the A_s-peak at $\theta_{\text{inc}} = 44.6°$ is independent of $L_{\text{STF}} \geq 8\Omega$. The plots of A_p in Fig. 5(b) show that the DT wave at $\theta_{\text{inc}} = 44.6°$ can be excited by p-polarized incident plane waves as well. We have verified that these conclusions also hold for $L_d \in \{180, 220\}$ nm. Accordingly, we conclude that linearly polarized light can excite DT waves and sense the refractive index variation.

4. CONCLUDING REMARKS

Our numerical studies have demonstrated that the excitation of DT waves guided by the planar interface of an isotropic homogeneous dielectric material and a porous chiral STF could be used for optical sensing, with comparable sensitivity as that of the SPP-waves-based sensors with the same prism and chiral STF [19].

REFERENCES

1. A. D. Boardman, ed., *Electromagnetic Surface Modes* (Wiley, 1982).
2. J. A. Polo, Jr., T. G. Mackay, and A. Lakhtakia, *Electromagnetic Surface Waves: A Modern Perspective* (Elsevier, 2013).
3. R. J. Green, R. A. Frazier, K. M. Shakesheff, M. C. Davies, C. J. Roberts, and S. J. B. Tendler, "Surface plasmon resonance analysis of dynamic biological interactions with biomaterials," Biomaterials **21**, 1823–1835 (2000).
4. J. Homola, I. Koudela, and S. S. Yee, "Surface plasmon resonance sensors based on diffraction gratings and prism couplers: sensitivity comparison," Sens. Actuat. B: Chem. **54**, 16–24 (1999).
5. I. Abdulhalim, M. Zourob, and A. Lakhtakia, "Surface plasmon resonance for biosensing: a mini-review," Electromagnetics **28**, 214–242 (2008).
6. S. K. Arya, A. Chaubey, and B. D. Malhotra, "Fundamentals and applications of biosensors," Proc. Ind. Nat. Acad. Sci. **72**, 249–266 (2006).
7. J. H. T. Luong, K. B. Male, and J. D. Glennon, "Biosensor technology: technology push versus market pull," Biotechnol. Adv. **26**, 492–500 (2008).
8. S. E. Swiontek, D. P. Pulsifer, and A. Lakhtakia, "Optical sensing of analytes in aqueous solutions with a multiple surface-plasmon-polariton-wave platform," Sci. Rep. **3**, 1409 (2013).
9. P. Yeh, A. Yariv, and C.-S. Hong, "Electromagnetic propagation in periodic stratified media. I. General theory," J. Opt. Soc. Am. **67**, 423–438 (1977).
10. P. Yeh, A. Yariv, and A. Y. Cho, "Optical surface waves in periodic layered media," Appl. Phys. Lett. **32**, 104–105 (1978).
11. M. Shinn and W. M. Robertson, "Surface plasmon-like sensor based on surface electromagnetic waves in a photonic bandgap material," Sens. Actuat. B **105**, 360–364 (2005).
12. V. N. Konopsky and E. V. Alieva, "Photonic crystal surface waves for optical biosensors," Anal. Chem. **79**, 4729–4735 (2007).
13. P. Rivolo, F. Michelotti, F. Frascella, G. Digregorio, P. Mandracci, L. Dominici, F. Giorgis, and E. Descrovi, "Real time secondary antibody detection by means of silicon-based multilayers sustaining Bloch surface waves," Sens. Actuat. B: Chem. **161**, 1046–1052 (2012).
14. A. Lakhtakia and J. A. Polo, Jr., "Dyakonov-Tamm wave at the planar interface of a chiral sculptured thin film and an isotropic dielectric material," J. Eur. Opt. Soc. Rapid Pub. **2**, 07021 (2007).
15. D. P. Pulsifer, M. Faryad, and A. Lakhtakia, "Observation of the Dyakonov-Tamm wave," Phys. Rev. Lett. **111**, 243902 (2013).
16. D. P. Pulsifer, M. Faryad, A. Lakhtakia, A. S. Hall, and L. Liu, "Experimental excitation of the Dyakonov–Tamm wave in the grating-coupled configuration," Opt. Lett. **39**, 2125–2128 (2014).
17. A. Lakhtakia and M. Faryad, "Theory of optical sensing with Dyakonov–Tamm waves," J. Nanophoton. **8**, 083072 (2014).
18. A. Lakhtakia and R. Messier, *Sculptured Thin Films: Nanoengineered Morphology and Optics* (SPIE, 2005).
19. T. G. Mackay and A. Lakhtakia, "Modeling chiral sculptured thin films as platforms for surface-plasmonic-polaritonic optical sensing," IEEE Sens. J. **12**, 273–280 (2012).
20. I. J. Hodgkinson, Q. h. Wu, and J. Hazel, "Empirical equations for the principal refractive indices and column angle of obliquely-deposited films of tantalum oxide, titanium oxide and zirconium oxide," Appl. Opt. **37**, 2653–2659 (1998).
21. N. S. Kapany and J. J. Burke, *Optical Waveguides* (Academic, 1972).